0026-895X/05/6805-1455–1465$20.00
MOLECULAR PHARMACOLOGY
Copyright © 2005 The American Society for Pharmacology and Experimental Therapeutics
Mol Pharmacol 68:1455–1465, 2005

Vol. 68, No. 5
16576/3060273
Printed in U.S.A.

Analysis of Human Multidrug Resistance Protein 1 (ABCC1) by Matrix-Assisted Laser Desorption Ionization/Time of Flight Mass Spectrometry: Toward Identification of Leukotriene C_4 Binding Sites

Peng Wu, Curtis J. Oleschuk,[1] Qingcheng Mao,[2] Bernd O. Keller, Roger G. Deeley, and Susan P. C. Cole

Division of Cancer Biology and Genetics, Cancer Research Institute (P.W., Q.M., R.G.D., S.P.C.C.), Department of Pharmacology and Toxicology (C.J.O., S.P.C.C.), and Department of Chemistry (B.O.K., S.P.C.C.), Queen's University, Kingston, Ontario, Canada

Received July 12, 2005; accepted August 15, 2005

ABSTRACT

Multidrug resistance in tumor cells may be caused by reduced drug accumulation resulting from expression of one or more proteins belonging to the ATP-binding cassette (ABC) transporter superfamily. In addition to their drug efflux properties, certain ABC proteins such as multidrug resistance protein 1 (MRP1) (ABCC1) mediate the ATP-dependent transport of a broad array of organic anions. The intrinsically photoreactive glutathione-conjugated cysteinyl leukotriene C_4 (LTC_4) is a high-affinity physiological substrate of MRP1 and is widely regarded as a model compound for evaluating the substrate binding and transport properties of wild-type and mutant forms of the transporter. In the present study, we have optimized high-level expression of recombinant human MRP1 in *Pichia pastoris* and developed a two-step purification scheme that results in purification of the transporter to >90% homogeneity. Peptide mapping by matrix-assisted laser desorption ionization/time of flight mass spectrometry of the peptides generated by in-gel protease digestions of purified underglycosylated MRP1 identified 96.7% of the MRP1 sequence with >98% coverage of its 17 transmembrane helices. Subsequent comparisons with mass spectra of MRP1 photolabeled with LTC_4 identified six candidate LTC_4-modified peptide fragments that are consistent with the conclusion that the intracellular juxtamembrane positions of transmembrane helices 6, 7, 10, 17, and a COOH-proximal portion of the cytoplasmic loop that links the first and second membrane spanning domains are part of the LTC_4 binding site of the transporter. Our studies confirm the usefulness of mass spectrometry for analysis of mammalian polytopic membrane proteins and for identification of substrate binding sites of human MRP1.

Resistance to anticancer agents remains a major cause of chemotherapeutic failure in patients with malignant diseases. One widely accepted mechanism of resistance is the active extrusion of drugs out of cells by membrane transport proteins, resulting in cellular drug levels below the threshold needed for cytotoxicity (Haimeur et al., 2004b). Numerous clinical and in vitro studies have established that multidrug resistance may be caused by enhanced expression of one or more proteins belonging to the ABC transporter superfamily that use the energy provided by ATP binding and hydrolysis at their nucleotide binding domains (NBDs) to power the transport of substrates across biological membranes.

MRP1 (ABCC1) belongs to the "C" branch of ABC transporters and was originally identified based on its elevated expression in a multidrug-resistant lung cancer cell line

This work was supported by a grant from the Canadian Institutes of Health Research (CIHR, MOP-10519). The mass spectrometry facility in the Department of Chemistry is funded by the Canadian Foundation for Innovation (Project 4989). C.J.O. is recipient of a CIHR Doctoral Award and Ontario Graduate Scholarship. R.G.D. is a Stauffer Research Professor at Queen's University. S.P.C.C. is Canada Research Chair in Cancer Biology and Senior Scientist of Cancer Care Ontario.

[1] Current affiliation: Department of Pathology and Molecular Medicine, McMaster University Medical Centre, Hamilton, ON, Canada.

[2] Current affiliation: Department of Pharmaceutics, University of Washington, Seattle, WA.

Article, publication date, and citation information can be found at http://molpharm.aspetjournals.org.
doi:10.1124/mol.105.016576.

ABBREVIATIONS: ABC, ATP-binding cassette; NBD, nucleotide binding domain; MRP1, multidrug resistance protein 1; MSD, membrane spanning domain; CL, cytoplasmic loop; TM, transmembrane; [^{125}I]AALTC_4, [^{125}I]iodoarylazido-derivatized analog of LTC_4; GSH, glutathione; LTC_4, leukotriene C_4; PMSF, phenylmethylsulfonyl fluoride; LPG, lysophosphatidyl glycerol; DDM, *n*-dodecyl β-D-maltoside; Co^{2+}-IMAC, Co^{2+}-immobilized metal affinity chromatography; 4-HCCA, α-cyano-4-hydroxycinnamic acid; DTT, dithiothreitol; PAGE, polyacrylamide gel electrophoresis; mAb, monoclonal antibody; MALDI-TOF, matrix-assisted laser desorption ionization/time of flight; PNGase F, *N*-glycosidase F; CHAPS, 3-[(3-cholamidopropyl)dimethylammonio]propanesulfonate.

(Cole et al., 1992). In tumor cells, MRP1 confers resistance to a broad range of antineoplastic drugs, whereas in normal tissues, MRP1 serves a protective role against these and other cytotoxic agents (Haimeur et al., 2004b; Leslie et al., 2005). A typical mammalian ABC protein has a four-domain structure with two membrane spanning domains (MSDs) and two NBDs. However, MRP1 contains a third MSD at its NH_2 terminus that is linked to the four-domain core by a cytoplasmic loop, CL3 (also referred to as L0), of approximately 125 amino acids. Thus, the 1531 amino acid MRP1 contains 17 transmembrane (TM) helices distributed among three MSDs configured MSD-CL3-MSD-NBD1-MSD-NBD2 (Haimeur et al., 2004b).

In addition to anticancer drugs, many of the chemicals transported by MRP1 are organic anions that include GSH, glucuronate, and sulfate conjugates that are not transported by the well known but distantly related drug transporter P-glycoprotein (ABCB1) (Haimeur et al., 2004b; Leslie et al., 2005). Most studies to date suggest that the first contacts of the hydrophilic amphipathic substrates of MRP1 are amino acids located in the inner leaflet of the membrane or in proximity to the cytosol-membrane interface of the two core MSDs of the transporter . The best characterized organic anion substrate of MRP1 in vitro is the cysteinyl leukotriene LTC_4 that is formed by conjugation of LTA_4 with GSH during inflammatory and immunological responses (Leier et al., 1994; Muller et al., 1994; Loe et al., 1996; Mao et al., 2000). Analyses of *Mrp1*$^{-/-}$ knockout mice have confirmed that LTC_4 is an endogenous substrate of MRP1 in vivo (Wijnholds et al., 1997). LTC_4 has a high-affinity (K_m of ~100 nM) for MRP1 and is also intrinsically photoreactive (Leier et al., 1994; Loe et al., 1996). Therefore, LTC_4 has been widely used as a model substrate to evaluate the substrate binding and transport properties of MRP1 (Bakos et al., 1998; Cai et al., 2001; Qian et al., 2001; Haimeur et al., 2002; Lee and Altenberg, 2003b; Yang et al., 2003).

In previous studies, we showed that both the second and third MSDs of MRP1 can be photolabeled by [^{3}H]LTC_4, with significantly more of the radioactivity associated with the NH_2-proximal half of the transporter (Qian et al., 2001). We also determined that a significant portion of CL3 is a prerequisite for efficient LTC_4 binding to the NH_2-terminal half of the protein, although neither this region nor the first MSD are themselves radiolabeled by the tritiated cysteinyl leukotriene. In addition, site-directed mutagenesis studies have identified a number of mutation-sensitive amino acids with respect to transport and/or binding of LTC_4. Thus, nonconservative (and in some cases, conservative) substitutions of certain residues located in or proximal to the cytosolic interface of TM6 (Lys^{332}, Asp^{336}), TM8 (Asp^{436}), TM11 (Asn^{590}, Arg^{593}, Phe^{594}, Pro^{595}), TM16 (Arg^{1197}), and TM17 (Arg^{1249}) eliminate or substantially decrease LTC_4 binding to the transporter (Haimeur et al., 2002, 2004a; Campbell et al., 2004; Koike et al., 2004; Situ et al., 2004; Zhang et al., 2004). However, it is not known whether these amino acids are in direct contact with LTC_4 or whether they have an indirect but critical role in maintaining the architecture of the LTC_4 binding site on the protein, or both.

Progress in elucidating the substrate binding sites and transport mechanism of MRP1 and other mammalian ABC proteins has been hampered by the lack of high-resolution crystal structures. Mass spectrometry is a complementary approach to identifying substrate or inhibitor binding sites on proteins that has been used with increasing success in recent years. However, their hydrophobicity and propensity to aggregate has limited the analysis of integral membrane proteins by this method. On the other hand, the feasibility of detailed mass spectrometric analysis has been enhanced by recent improvements in large-scale production of mammalian membrane proteins as well as advances in solubilization, purification, and proteolytic digestion methods (Washburn et al., 2001; Quach et al., 2003; Eichacker et al., 2004). Nevertheless, complete sequence coverage of large polytopic mammalian proteins such as MRP1 by mass spectrometry remains rare. In the current study, we have explored the feasibility of using mass spectrometry to better define how MRP1 interacts with LTC_4.

Materials and Methods

Chemicals and Reagents. The *Pichia pastoris* strain KM71 transformed with plasmid pHIL-MRP1-cHA-His_6 was a generous gift of Drs. Philippe Gros and Jie Cai (McGill University, Montreal, QC, Canada) (Cai et al., 2001). Leupeptin and aprotinin were from Roche Diagnostics (Indianapolis, IN). PMSF and pepstatin A were from ICN (MP Biomedicals, Aurora, OH), and LPG was from Avanti Polar Lipids (Alabaster, AL). DDM, chymotrypsin (protein and peptide sequencing grade), protease V8 (protein and peptide sequencing grade), and 4-HCCA were from Sigma-Aldrich (St. Louis, MO). Trypsin Gold (mass spectrometry grade) was from Promega (Madison, WI). BD Talon superflow Co^{2+}-IMAC resins were from BD Biosciences Clontech (Palo Alto, CA). Preswollen microgranular anion exchange DE52 DEAE cellulose was from Whatman (Maidstone, UK). [14,15,19,20-^{3}H]LTC_4 (115.3 Ci/mmol) was from GE Healthcare (Little Chalfont, Buckinghamshire, UK). LTC_4 was from Calbiochem (San Diego, CA). Other chemicals were high-performance liquid chromatography or analytical grade unless specified otherwise.

Large-Scale Expression of MRP1 in *P. pastoris*. Large-scale expression of MRP1 in *P. pastoris* was carried out in baffled flasks at 28–30°C essentially as described by the manufacturer (Invitrogen, Carlsbad, CA). In brief, a single colony was inoculated in 50 ml of MGY (1.34% yeast nitrogen base with ammonium sulfate, 1% glycerol, and 4×10^{-5}% biotin) in a 250-ml flask and incubated at 28–30°C and 250 to 275 rpm overnight. Ten milliliters of cultured cells was transferred into 1 liter of MGY and further incubated to an optical density at 600 nm of 2.0 to 6.0. Cells were collected by centrifugation and resuspended in the same volume of MM (1.34% yeast nitrogen base with ammonium sulfate, 0.5% methanol, and 4×10^{-5}% biotin) to induce MRP1 expression. Cell growth was then continued for a further 3 days, and methanol was added to a final concentration of 0.5% every 24 h to maintain induction. Finally, cells were collected by centrifugation and washed three times with ice-cold homogenization buffer (300 mM Tris-HCl, 250 mM sucrose, 100 mM ϵ-aminocaproic acid, 1 mM EDTA, 1 mM EGTA, and 1 mM DTT, pH 7.4) at 1500*g* for 15 min at 4°C. Cell pellets were snap-frozen in liquid N_2 and stored at −80°C.

Preparation of Crude Membranes. Yeast cells were diluted 50% (v/v) in homogenization buffer containing protease inhibitors (1 mM PMSF, 10 μg/ml pepstatin A, 10 μg/ml leupeptin, and 2 μg/ml aprotinin) and then disrupted three times using a French pressure cell press (Thermo Electron Corporation, Waltham, MA) set at 20,000 psi; fresh PMSF (1 mM) was added after each interval. After centrifugation, the pellet was washed twice, and supernatants were pooled and centrifuged at 100,000*g* for 60 min. The resulting membrane pellet was homogenized vigorously with a motor-driven homogenizer in resuspension buffer (50 mM Tris-HCl, 20% glycerol, 10 mM imidazole, and 1 mM 2-mercaptoethanol, pH 8.0). The crude microsomes were recentrifuged and rehomogenized twice as de-

scribed above. The resulting crude membrane proteins were stored at −80°C in resuspension buffer containing protease inhibitors. Protein concentrations were determined using a Bradford assay using bovine serum albumin as a standard.

Purification of MRP1. Crude membrane proteins were thawed and diluted to 5.0 mg/ml in resuspension buffer containing protease inhibitors. In general, 100 mg of membrane proteins was solubilized by addition of LPG (4–6 mg/ml) followed by inversion for 2 to 3 h at 4°C. Insoluble proteins were removed by centrifugation at 100,000*g* for 20 min at 4°C. The supernatant were diluted 3-fold by addition of resuspension buffer containing protease inhibitors, 0.8 M NaCl, and 0.187 mg/ml DDM to minimize the interaction of LPG with Co^{2+}-IMAC resin. Co^{2+}-IMAC resin (100 μl/mg membrane protein) that had been pre-equilibrated in resuspension buffer containing DDM was added to the diluted supernatant. The slurry was incubated at room temperature for 1 to 2 h with continuous inversion and then transferred into a Bio-Rad column (1 × 35 cm). The resin was washed extensively with five to 10 bed volumes of resuspension buffer and followed by 20 bed volumes of washing buffer (50 mM Tris-HCl, 0.8 M NaCl, 20% glycerol, 20 mM imidazole, 1 mM 2-mercaptoethanol, and 0.187 mg/ml DDM, pH 8.0). The bound MRP1 was eluted with elution buffer (50 mM Tris-HCl, 450 mM NaCl, 20% glycerol, 200 mM imidazole, 1 mM 2-mercaptoethanol, and 0.187 mg/ml DDM, pH 7.4) containing protease inhibitors. Proteins in each fraction were analyzed by 7% SDS-PAGE followed by silver staining. Fractions containing MRP1 were pooled and dialyzed against storage buffer (50 mM Tris-HCl, 10% glycerol, 1 mM 2-mercaptoethanol, and 0.187 mg/ml DDM, pH 8.0). MRP1 was further purified by adding the dialyzed protein to DE52 anion exchange resin pre-equilibrated in storage buffer and incubated for 1 h at 4°C. The supernatant was removed by centrifugation and purified MRP1 was eluted with 400 mM NaCl in storage buffer by centrifugation at 3500*g* for 5 min at 4°C and then stored in aliquots at −80°C.

Immunoblot Analysis of MRP1. Protein samples (15 μg of crude membranes; 0.5 μg of purified MRP1) were resolved by SDS-PAGE and transferred to an Immobilon-P membrane (Millipore Corporation, Billerica, MA). MRP1 was routinely detected using mAb QCRL1 (epitope residues 918–924) (Hipfner et al., 1996). Antibody binding was detected with a horseradish peroxidase-conjugated secondary antibody and the signal was enhanced using Renaissance chemiluminescence reagent (PerkinElmer Life and Analytical Sciences, Boston, MA) and exposed to film. Relative levels of MRP1 were determined by densitometry of the films using ImageJ 1.32j software (http://rsb.info.nih.gov/ij/index.html).

Photolabeling of Purified MRP1 with LTC_4 and [^{3}H]LTC_4. Purified MRP1 in buffer (50 mM Tris-HCl, 250 mM sucrose, and 0.187 mg/ml DDM, pH 7.4) containing 50 or 100 mM $MgCl_2$ was incubated with unlabeled and/or ^{3}H-labeled LTC_4 at room temperature for 30 min and then frozen in liquid N_2. LTC_4 was cross-linked to MRP1 by alternately irradiating the mixture at 302 nm for 1 min using a CL-1000 Ultraviolet Crosslinker (DiaMed, Mississauga, ON, Canada) and snap-freezing in liquid N_2 10 times. LTC_4-labeled MRP1 was resolved by SDS-PAGE, and gels containing [^{3}H]LTC_4-labeled MRP1 were processed for autoradiography at −80°C (Loe et al., 1996). Relative levels of photolabeled MRP1 were determined by densitometry as described above.

In-Gel Proteolytic Digestions of Unlabeled and [^{3}H]LTC_4-Labeled MRP1. Trypsin, chymotrypsin, and protease V8 were used alone or in combination for in-gel digestions of MRP1, first as the unlabeled protein, and subsequently after photolabeling with LTC_4. After a series of initial experiments, a protocol was developed as follows (Fig. 2). Unlabeled or LTC_4-labeled MRP1 was incubated with 20 mM DTT in 100 mM NH_4HCO_3, pH 7.8, for 45 min at 37°C and then carbamidomethylated by incubation with freshly prepared 45 mM iodoacetamide in 100 mM NH_4HCO_3, pH 7.8, in the dark for 20 min. After SDS-PAGE, protein bands at ~165 kDa were cut into small slices and transferred to siliconized tubes. The gel pieces were washed three times with water and five times with 50% acetonitrile in 100 mM NH_4HCO_3, dehydrated in 100% acetonitrile, and then taken to dryness in a SpeedVac (Thermo Electron). The dried gel pieces were reswollen and incubated with 40 μl of trypsin (20 ng/ml, pH 7.8), chymotrypsin (5 ng/ml, pH 7.8), or protease V8 (6 ng/ml, pH 6.5) overnight at 37°C. When more than one proteolytic digestion was performed, the first digested peptide mixture was adjusted to the optimal incubation conditions for the second enzyme. Thereafter, 1 μl of the second enzyme [trypsin (100 ng/ml, pH 7.8), chymotrypsin (25 ng/ml, pH 7.8), or protease V8 (30 ng/ml, pH 6.5)] was added followed by incubation for 4 h at 37°C. The peptide fragments were extracted three times by sonication at room temperature for 10 min with 50% acetonitrile and 0.2% trifluoroacetic acid. All extracts were pooled and concentrated by Speed Vac before analysis by mass spectrometry.

MALDI-TOF Mass Spectrometry. Samples for MADLI-TOF analyses were prepared using the two-layer deposition method (Dai et al., 1999). In brief, 1 μl of thin layer matrix solution (6 mg/ml 4-HCCA in 70% acetone and 30% methanol) was deposited on a clean target, where the solution spread and evaporated rapidly. The digested peptides were mixed with an equal volume of thick layer matrix solution (4-HCCA saturated in 60% methanol), and 0.5 μl of this mixture was deposited on top of the first layer and allowed to air dry. Samples were rinsed by placing deionized water (0.5 μl) on the sample matrix surface for 20 s and then blown off with N_2. This washing procedure was repeated three times.

Mass spectra were recorded using a Voyager DE STR MALDI-TOF mass spectrometer (Applied Biosystems, Foster City, CA), equipped with a standard nitrogen laser (337 nm). All mass spectra were collected in positive mode with delayed extraction and reflectron mode. The sample spot was scanned with the laser beam under video observation, and spectra were acquired by averaging 200 to 500 individual laser shots and processed with Data Explorer software (Applied Biosystems). The spectra were internally calibrated with matrix peaks and enzyme autolysis peptide peaks. Known contaminant peak signals were removed from the resulting data and remaining sample peak signals used for database searching. The artificial modifications of peptides (carbamidomethylation of cysteines and partial oxidation of methionines) were also considered for the database searching. Peptide identification and sequence coverage were interpreted against the SwissProt.10.30.2003 protein database with the aid of three scoring algorithm programs: Protein Prospector (http://prospector.ucsf.edu/), Mascot (http://www.matrixscience.com/search_form_select.html), and FindPept (http://ca.expasy.org/tools/findpept.html).

Results

Large-Scale Production and Characterization of MRP1 in *P. pastoris*. Large-scale expression of recombinant full-length MRP1-His_6 was carried out using *P. pastoris* strain KM71 (*arg4*, *his4 aox1*::*ARG4*, Mut^s) (Cai et al., 2001). A typical preparation yielded 85 mg of crude membranes per 1liter of yeast medium. MRP1 levels were determined by immunoblotting of the membranes, and a major immunoreactive band of ~165 kDa was observed (Fig. 1A). The intensity of this band was comparable with that observed for an equivalent amount of membrane proteins from the human H69AR lung cancer cell line, the differences in electrophoretic mobility being attributed to differences in glycosylation. Because MRP1 is known to make up approximately 5 to 6% of total H69AR membrane proteins (Mao et al., 1999, 2000), this indicates that the recombinant MRP1 accounts for a comparable proportion of the yeast membrane proteins.

When *P. pastoris* crude membranes enriched for MRP1 were treated with PNGase F, the electrophoretic mobility of the immunoreactive band was not altered (Fig. 1A). In con-

trast, PNGase F treatment of H69AR cell membranes reduced the apparent molecular mass of native MRP1 from 190 kDa to a mass similar to that of the recombinant MRP1 expressed in *P. pastoris*, confirming that human MRP1 expressed in the latter system is underglycosylated (Cai et al., 2001). Uptake assays using membrane vesicles prepared from *P. pastoris* cells expressing MRP1 confirmed that the recombinant protein could transport LTC_4 as well as reported previously (Cai et al., 2001).

Purification of Unlabeled MRP1 Expressed in *P. pastoris*. Solubilization of MRP1 from crude membranes prepared from *P. pastoris* cells was evaluated initially using several detergents followed by immunoblotting with mAb QCRL-1. CHAPS and taurocholic acid were ineffective, whereas ~50% of MRP1 was solubilized by DDM or lysophosphatidylcholine using a detergent/protein ratio of >6. LPG was more effective than either DDM and lysophosphatidylcholine and solubilized >90% of MRP1 at a relatively low detergent/protein ratio and at 4°C (data not shown). It is worth noting that it was necessary to exclude NaCl during solubilization by LPG to avoid precipitation of the detergent. LPG did not interfere with binding of the recombinant MRP1 to Co^{2+}-chelated Sepharose resin but did seem to reduce its affinity for the Co^{2+}-IMAC resin. Therefore, LPG-solubilized MRP1 was diluted with DDM-containing buffer before mixing with the Co^{2+}-IMAC resin. Use of DDM afforded the additional advantage of being a nonionic detergent and thus far less likely than LPG to interfere with ionization of peptides from the MALDI matrix (Reid, 2004).

Purification of MRP1 by Co^{2+}-IMAC was followed by SDS-PAGE, and the protein was visualized by silver staining. In this way, MRP1 was purified to ~50% homogeneity with a single contaminating band at ~55 kDa (Fig. 1B). This latter band was not detected with three MRP1-specific mAbs directed against epitopes in three different regions of the transporter (data not shown), indicating that the impurity was not an MRP1 degradation product and was probably a copurifying protein from the yeast host.

After Co^{2+}-IMAC, MRP1 was further purified to >90% homogeneity using DE52 anion chromatography (Fig. 1C). The overall yield of purified MRP1 obtained from 1.0 l of yeast medium was ~400 μg. This represents a 2-fold higher yield than that previously reported using a *Saccharomyces cerevisiae* expression system (Lee and Altenberg, 2003b). The purified recombinant MRP1 could be photolabeled with [^{3}H]LTC_4 (see below) and 8-azido-[α-^{32}P]ATP, and it had a substantial amount of intrinsic ATPase activity, indicating the protein had retained its activity through the purification process (data not shown).

In-Gel Proteolytic Digestion and MALDI-TOF Analysis of Unlabeled MRP1. To assess the feasibility of identifying MRP1 LTC_4 binding sites by MALDI TOF, intact

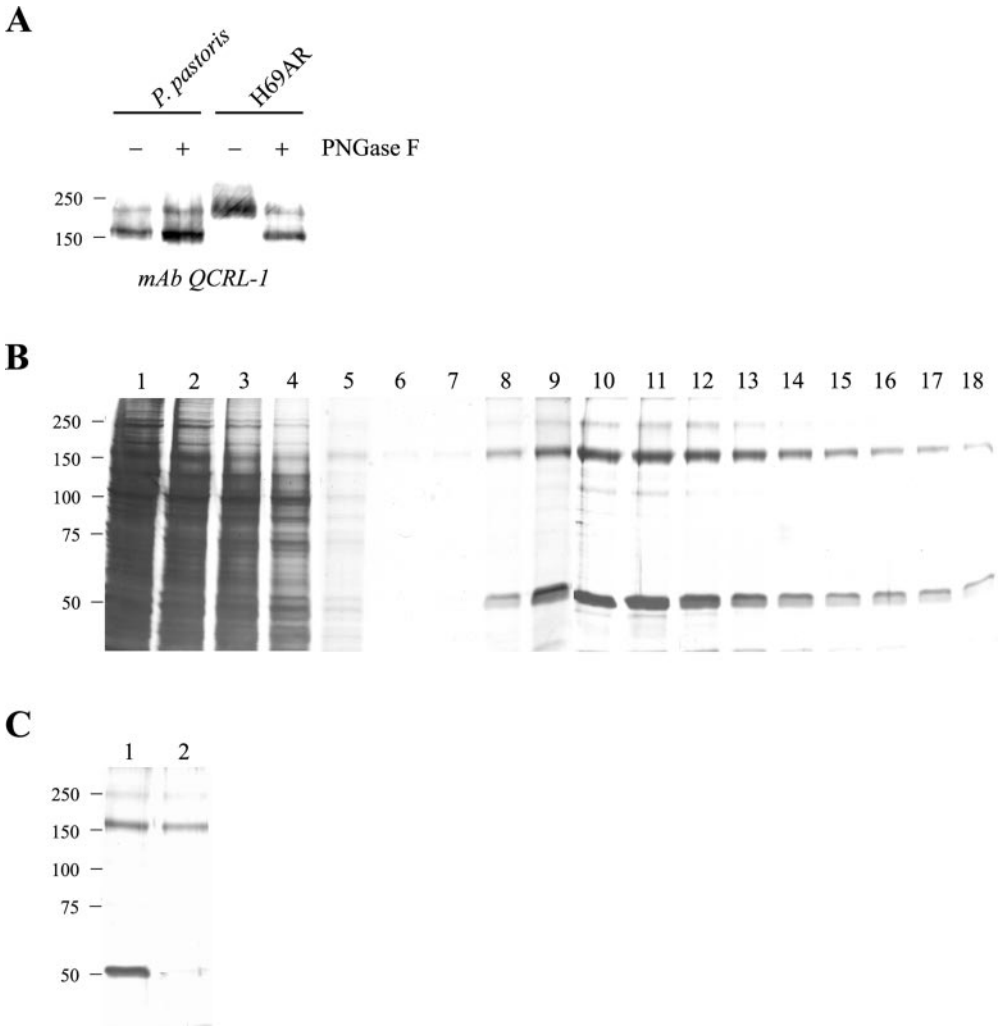

Fig. 1. Expression and purification of recombinant human MRP1 in *P. pastoris*. A, immunoblot of MRP1-enriched membranes prepared from *P. pastoris* cells and human H69AR lung cancer cells with mAb QCRL-1 after treatment with PNGase F. Crude membrane proteins (20 μg) were incubated at 37°C for 1 to 2 h in the absence (−) or presence (+) of PNGase F, and MRP1 proteins detected by immunoblotting with mAb QCRL-1. B, purification of MRP1 by Co^{2+}-IMAC was monitored by SDS-PAGE, and proteins were visualized by silver staining. Lane 1, unstained protein standards; lane 2, LPG-solubilized crude membrane proteins (2 μl); lane 3, supernatant of LPG-solubilized protein (2 μl); lane 4, flow-through from Co^{2+}-IMAC column (2 μl); lane 5, eluate from first wash of Co^{2+}-IMAC column with resuspension buffer (20 μl); lane 6, eluate from second wash of column with washing buffer (20 μl); and lanes 7 to 18, sequential fractions of column eluates with 200 mM imidazole (20 μl). C, silver-stained gel after typical two-step purification of MRP1 by Co^{2+}-IMAC and DE52 anion chromatography. Lane 1, DDM-solubilized and dialyzed MRP1 after Co^{2+}-IMAC (20 μl); and lane 2, eluate after DE52 chromatography with 400 mM NaCl (20 μl). Molecular mass markers are shown on the left.

unlabeled purified MRP1 was first digested with a variety of conventional proteases and chemicals, and the resulting fragments were analyzed by MALDI-TOF mass spectrometry. DDM was routinely required during sample concentration and MALDI matrix crystal formation to maintain solubility. In contrast to analysis of the bacterial lactose transporter LacS (Van Montfort et al., 2002), treatment of MRP1 with trypsin and cyanogen bromide yielded relatively few identifiable peptides, and of these, even fewer corresponded to predicted TM helices (data not shown). To increase sequence coverage, a protocol was developed that ultimately led to identification of 96.7% of the MRP1 sequence (Fig. 2); of this, 98.8% of the TM sequences in the two core MSDs were identified (Table 1). Important modifications included subjecting the protein to reducing and carbamidomethylating conditions before separation by SDS-PAGE, and sequential use of two proteases. Thus, MRP1 was first digested with trypsin, chymotrypsin, or protease V8, and then the resulting peptide mixtures were subjected to a second digestion with a different enzyme, as outlined in Fig. 2.

The presence of unassignable mass peaks in MALDI TOF mass spectrometry is not uncommon, and such peaks were also found in our analyses (Ding et al., 2003). In general, contaminating peaks originate from matrix clusters, proteolytic autolysis, or human keratin. The peaks from matrix cluster (*m/z* 568.1), gel (*m/z* 882.5), proteolytic autolysis (*m/z* 2211.1 for trypsin), and some known peptides were used for internal mass calibration (Fig. 3). To avoid potential contamination from matrix, only mass peaks greater than *m/z* 700 were searched against the SwissProt.10.30.2003 protein database (Table 1). All searches were limited to the first monoisotopic peaks, and all cysteine residues were presumed to be reduced and carbamidomethylated, and partial oxidation of methionine residues was considered. Up to four missing enzyme cleavage sites were considered for single digests and for double digests, up to seven missing cleavage sites were considered.

As indicated in Table 1, more sequence coverage was obtained from single digestions with trypsin than from chymotrypsin or protease V8 digestions. Chymotrypsin digestion produced very short peptides, and as a result, many potential MRP1 peptides were artificially excluded during database searching. MRP1 digestion with protease V8 in NH_4HCO_3 yielded poorer correlations of mass spectra with MRP1 sequences (data not shown). This shortcoming was overcome by carrying out protease V8 digestions at pH 6.5. When protease V8 and chymotrypsin were used in combination, the resulting coverage of the MRP1 sequence was significantly greater than that obtained by digestion with each enzyme alone. In addition, the number of peptides obtained from a dual digestion depended on the order in which the proteases were added (Table 1). The reason for this is not known, but it may reflect differences in the accessibility of the cleavage sites in gel-trapped MRP1 to the proteases. After compiling sequences from multiple proteolytic digestions, it was clear that coverage of the MRP1 sequence was nearly complete, and included almost all of the TM helices. These experiments established the feasibility of identifying MRP1 substrate binding sites by MALDI-TOF mass spectrometry.

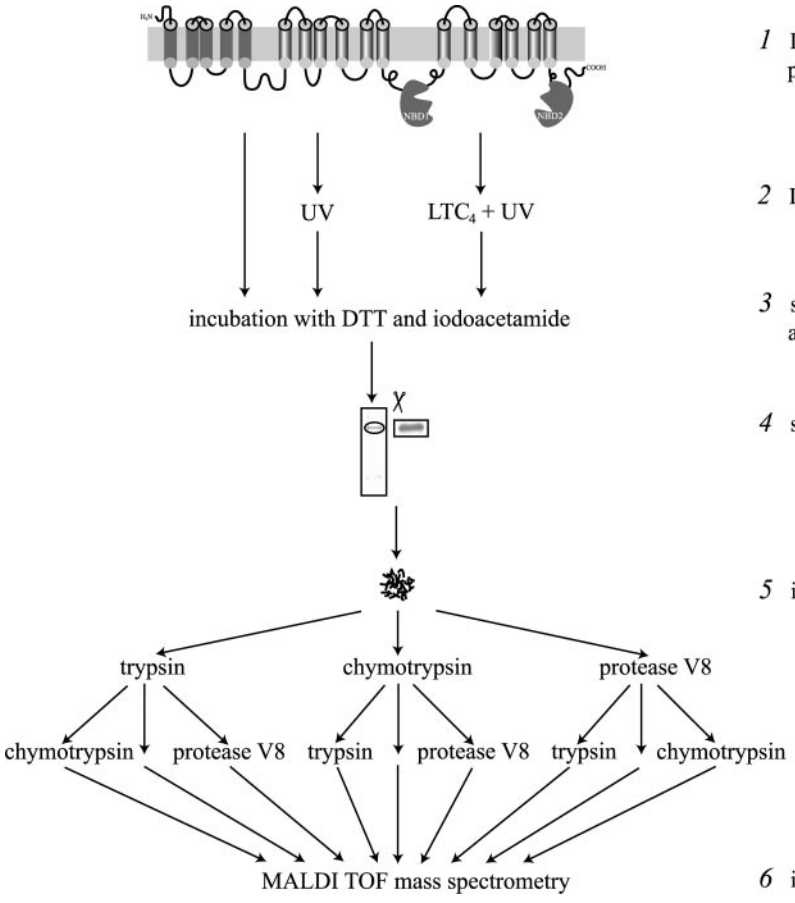

Fig. 2. Scheme showing experimental strategy for analysis of recombinant human MRP1 expressed in *P. pastoris* by MALDI-TOF. A six-step protocol for analysis of MRP1 with full-sequence coverage was developed as follows: 1, solubilization of purified recombinant MRP1 from *P. pastoris* in DDM. 2, photolabeling of purified MRP1 with LTC_4 by irradiation at 302 nm. Controls include unlabeled MRP1 and irradiated unlabeled MRP1. 3, treatment of MRP1 with DTT and iodoacetamide. 4, separation of unlabeled or LTC_4-labeled MRP1 by SDS-PAGE and excision of protein bands of ~165 kDa. 5, in-gel digestion of dried gel pieces with various combinations of proteases. 6, analysis of peptide fragments by MALDI-TOF mass spectrometry assisted by software programs MS-Fit, Mascot, and FindPept.

Photolabeling of Purified MRP1 with LTC_4. As mentioned previously, LTC_4 is intrinsically photoreactive, a property attributable to its conjugated triene structure (Fig. 4A) (Falk et al., 1989). In general, the efficiency of photochemical reactions is low and consequently, before mass spectrometry, conditions for optimal photolabeling with LTC_4 were determined by photolabeling a constant amount of purified MRP1 in increasing concentrations of [^{3}H]LTC_4. As shown in Fig. 4B, the extent of MRP1 photolabeling increased with increasing concentrations of LTC_4 until a maximum was reached at ~4 μM at which point the cysteinyl leukotriene was estimated to be in ~50-fold molar excess of MRP1.

Mass Spectrometry Analysis of LTC_4-Labeled MRP1. Purified MRP1 (typically 1 μg) was irradiated at 302 nm in the presence of LTC_4 (4 μM) as outlined in the protocol shown in Fig. 2. Controls included nonirradiated MRP1 and UV-irradiated MRP1 in the absence of LTC_4. MALDI-TOF analyses of all three samples showed several differences in terms of signal appearances (Fig. 5A). This is to be expected because MALDI-TOF is very sensitive to small differences in sample preparation or crystal formation, which in some cases can limit the usefulness of controls. In addition, UV irradiation of MRP1 can be expected to result in some degree of intra- or intermolecular cross-linking and/or other chemical reactions. However, because our goal was to identify LTC_4-modified peptides and because the formation of covalent bonds between LTC_4 and amino acid residues in MRP1 involves the opening of one or more of the triene double bonds during irradiation (Falk et al., 1989), those differences in the obtained spectra that did not match an exact mass shift of 625.5 Da from an unlabeled peptide to a LTC_4-labeled peptide were excluded from further consideration. In addition, the mass shifts were required to occur only for MRP1 irradiated in the presence of LTC_4 and not for the two controls.

Figure 5 shows an example of a positive match that meets the above-stated selection criteria and the properties of this and five other candidate LTC_4-modified peptide fragments are summarized in Table 2. These data suggest that the regions of MRP1 covalently bound to LTC_4 are preferentially located at the intracellular juxtamembrane positions of TM6,

TABLE 1
Relative sequence coverage of human MRP1 (ABCC1) identified by MALDI-TOF mass spectrometry

Protease	Total Sequence Coverage	MSD[a] (1–193)		CL3[a b] (194–322)	MSD[a c] (323–600)		NBD1[a d] (601–978)	MSD[a c] (979–1251)		NBD2[a d] (1252–1531)
		Loops	TMs		Loops	TMs		Loops	TMs	
	%									
Trypsin	39.3	14.8	20.0	54.3	47.1	24.3	44.6	28.2	18.9	59.3
Chymotrypsin	19.4	15.9	41.9	10.0	25.4	47.9	12.5	4.2	35.6	8.6
Protease V8	10.5	0.0	0.0	4.7	0.0	0.0	24.9	3.5	0.0	19.6
Trypsin + chymotrypsin	56.7	89.8	75.2	40.3	86.2	58.6	41.4	60.6	48.5	53.9
Trypsin + protease V8	48.7	47.7	20.0	38.8	63.8	12.1	69.8	26.1	24.2	70.4
Chymotrypsin + trypsin	59.6	64.8	89.5	86.8	79.0	54.3	40.1	62.0	64.4	50.4
Chymotrypsin + protease V8	42.5	56.8	55.2	50.4	42.0	52.9	36.9	41.5	46.2	26.4
Protease V8 + trypsin	43.5	23.9	20.0	66.7	64.5	0.0	52.8	43.0	43.2	47.1
Protease V8 + chymotrypsin	53.2	87.5	68.6	14.7	56.5	74.3	37.4	70.4	83.3	40.4

[a] The amino acids included in the MSDs, loops (cytoplasmic and extracellular), TMs, and NBDs are approximate and are based on predictions from atomic homology models of the second and third MSDs (Campbell et al., 2004) as well as the HMMTOP 2.0 algorithm.
[b] Overall coverage of CL3 was 100%.
[c] Overall coverage of two core MSDs (TM6–17) was 98.9% (only ^{590}NIL^{592} from TM11 was not identified).
[d] Overall coverage of Walker A, Walker B, and active transport C signature motifs was 100%.

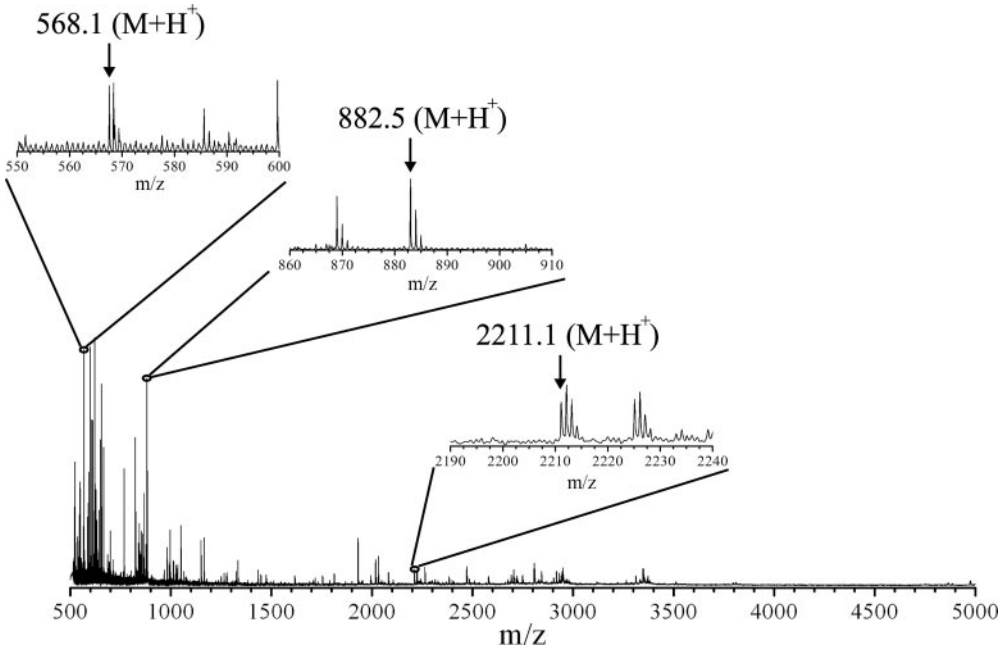

Fig. 3. Representative MALDI-TOF mass spectrum of in-gel trypsin digested unlabeled MRP1. Unlabeled purified MRP1 was resolved by SDS-PAGE, excised from the gel, and then the dried gel pieces were incubated with trypsin overnight at 37°C. Shown is a MALDI-TOF mass spectrum of the resulting tryptic peptides with expansion of the three main peaks used for internal calibration at *m/z* 568.1 (from matrix cluster), *m/z* 882.5 (from the gel), and *m/z* 2211.1 (from trypsin autolysis). Peaks at *m/z* 568.1 and *m/z* 882.5 were also observed in mass spectra of MRP1 digested with other proteases alone or in combination.

TM7, TM10, TM17, and in CL3 linking the first and second MSDs. The appearance of unlabeled peptide in the two controls as well as in the photolabeled sample is expected, because only a portion of the protein present is labeled in the photolabeling reaction.

Discussion

Despite many recent advances, analysis of polytopic mammalian membrane proteins by mass spectrometry and other biophysical methods still remains technically challenging (Glish and Vachet, 2003; Eichacker et al., 2004; Reid, 2004). Studies of human MRP1 and other mammalian ABC transporters have been further hampered by the difficulty of obtaining sufficiently large amounts of purified protein. Although MRP1 has been successfully purified to a high degree of homogeneity by several groups (Chang et al., 1997; Mao et al., 1999, 2000), the expression systems used to date are relatively inefficient, making it difficult and costly to generate the large amounts of protein needed for most biophysical studies. In contrast, the *P. pastoris* expression system can be readily scaled up and indeed, this system has been successfully applied to the large-scale production of a number of human polytopic membrane proteins, including P-glycoprotein (ABCB1) and the breast cancer resistance protein (ABCG2) (Cai and Gros, 2003; Mao et al., 2004).

When expressed in mammalian cells, MRP1 is *N*-glycosylated with complex carbohydrates at Asn residues at positions 19, 23, and 1006 (Hipfner et al., 1997), which has the potential to impede physical characterizations of the transporter. Indeed, the glycan chains of MRP1 have been reported by Muller et al. (2002) to impair the accessibility of its extracellular domains. Thus, another advantage of using *P. pastoris* is the fact that MRP1 expressed in this system is underglycosylated (Fig. 1) (Cai et al., 2001). Previous studies have shown that the absence of glycosylation does not cause any substantial alterations in the ability of MRP1 to transport LTC_4 (Gao et al., 1998), although in mammalian cells, the glycan chains may enhance the stability of the transporter (K. E. Weigl, R. G. Deeley, and S. P. C. Cole, unpublished observations).

By using a combination of DDM solubilization and Co^{2+}-IMAC and DE52 anion exchange chromatography, we were able to purify the recombinant MRP1 from *P. pastoris* membranes to >90% homogeneity. A typical yield from a 1-liter culture was ~400 μg, which is 2-fold higher than the yield reported previously for recombinant MRP1 using a heterologous *S. cerevisiae* expression system (Lee and Altenberg, 2003b). The DDM-solubilized purified MRP1 could be photolabeled with [^{3}H]LTC_4 and 8-azido-[α-^{32}P]ATP, and it also exhibited significant ATPase activity (data not shown). Thus, we can conclude that expression in *P. pastoris* together with our two-step purification protocol is a good system for obtaining substantial amounts of purified functional MRP1 that can be used with confidence for high-resolution structural analyses.

Previous studies indicate that many of the sites in MRP1 and other ABC proteins likely to interact directly with its xenobiotic and endogenous substrates are located in or at the cytosolic interface of its TM helices (Haimeur et al., 2004b). Thus, complete sequence coverage of the TMs is a critical prerequisite for identifying substrate contact sites on the transporter by mass spectrometry. Because of their hydrophobicity, this is often difficult to achieve with membrane proteins (Reid, 2004). Despite the fact that P-glycoprotein contains five fewer TMs than MRP1, Chiba and colleagues reported just 80% coverage of the human P-glycoprotein sequence by MALDI-TOF analysis in one study, and in a more recent study, 95% coverage of the two MSDs and 80% of the NBDs (Ecker et al., 2002; Pleban et al., 2005). Using our sequential protease digestion protocol, all residues in the TMs of the three MSDs of MRP1 were identified except for three amino acids in TM11, and the NBDs were 96.5% covered (Table 1). Thus, our MALDI-TOF analysis of human MRP1 with >96% overall sequence coverage represents a significant improvement and our protocol may facilitate the study of other large mammalian ABC transporters.

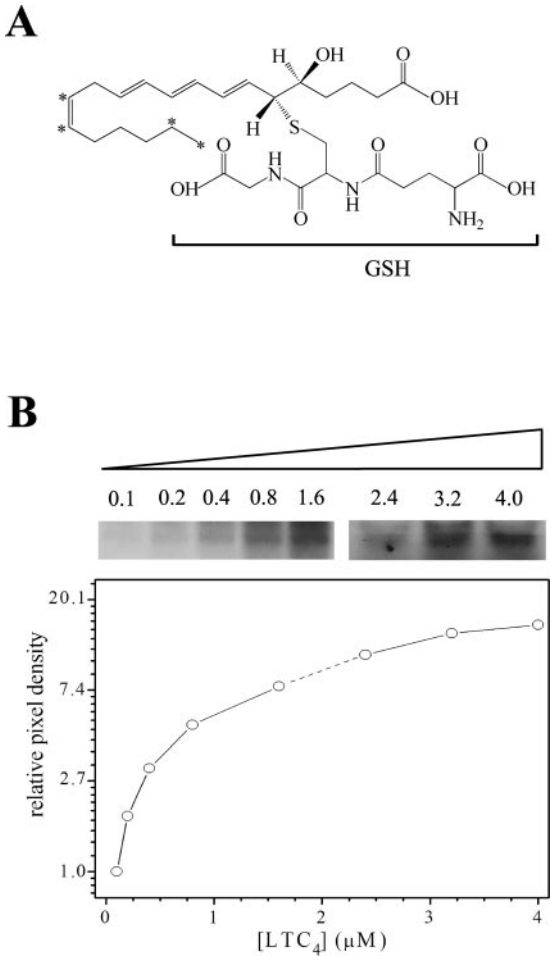

Fig. 4. Chemical structure of [^{3}H]LTC_4 and photolabeling of purified MRP1 with [^{3}H]LTC_4. A, chemical structure of [14,15,19,20-^{3}H]LTC_4. The asterisks indicate the location of the tritium atoms in the radiolabeled molecule. B, concentration dependence of LTC_4 photolabeling of MRP1. DDM-solubilized purified MRP1 (1.6 μg) was incubated with the indicated concentrations of [^{3}H]LTC_4/LTC_4 for 30 min at room temperature. After irradiating at 302 nm, the radiolabeled proteins were resolved by SDS-PAGE, processed for autoradiography, and the intensity of the bands quantified by densitometry. The figure is a composite of results obtained in two independent experiments, each with five different [^{3}H]LTC_4 concentrations (0.1, 0.2, 0.4, 0.8, and 1.6; and 0.8, 1.6, 2.4, 3.2, and 4.0). In the graph, the relative pixel densities for the second set of data were plotted after "correction" so that the signal intensities of the two overlapping concentrations (0.8 and 1.6) were the same. Therefore, the signals for these two [^{3}H]LTC_4 concentrations in the second experiment are not shown. The dotted line in the graph connects the data points from the two experiments.

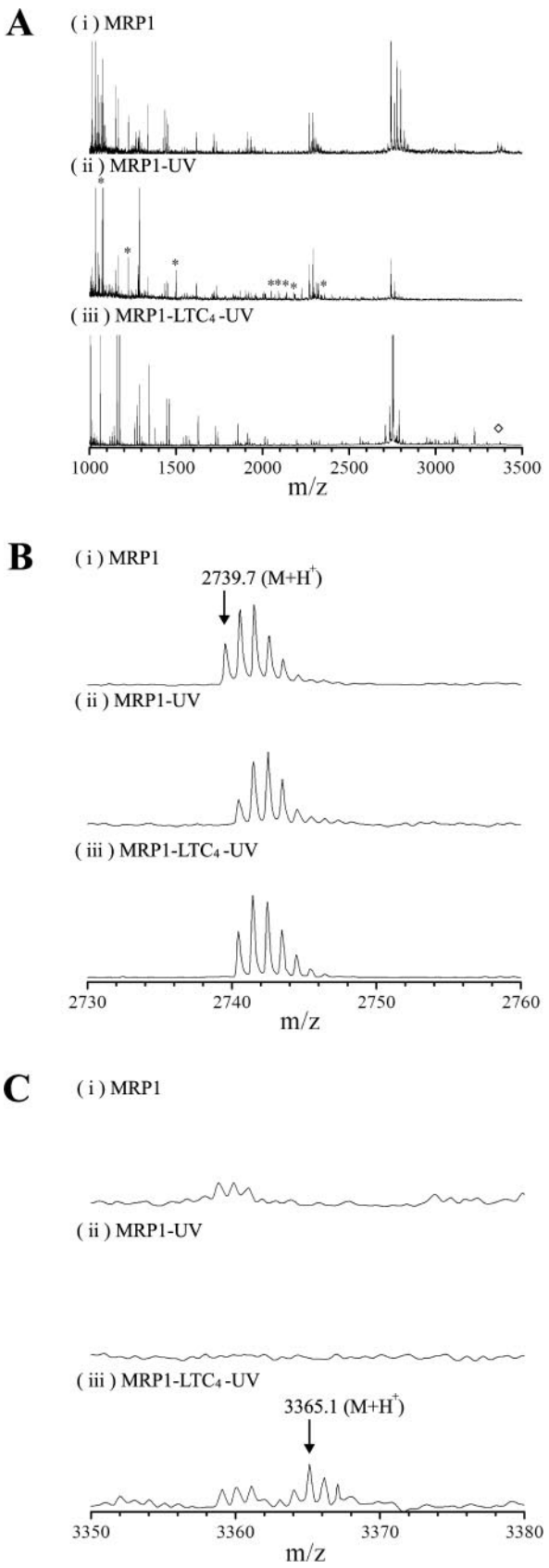

Fig. 5. Representative mass spectra identifying candidate LTC_4-modified peptides of MRP1. A to C, MALDI-TOF mass spectra of MRP1 digested with protease V8 and chymotrypsin. In all panels, i, unlabeled nonirradiated MRP1 (MRP1), ii, unlabeled irradiated MRP1 (MRP1-UV), and iii, LTC_4-photolabeled MRP1 (MRP1-LTC_4-UV). A, mass spectra of MRP1 peptides at *m/z* 1000 to 3500 obtained by in-gel digestion with protease V8 and chymotrypsin. Peaks marked with asterisks in ii are not detected in i and are attributed to differences in sample preparation or UV irradiation alone. The peak marked with a diamond in iii is candidate LTC_4-modified MRP1 peptide fragment. B and C, expanded sections of the mass spectra shown in A. B, the best match for the unmodified peptide at *m/z* 2739.7 is peptide 1233 to 1255 (Table 2). C, peptide at *m/z* 3365.1 is detected only in digests of LTC_4 cross-linked MRP1 (iii) and matches the unmodified peptide at *m/z* 2739.7 shown in B after subtraction of the mass of LTC_4. The *m/z* 2739.7 fragment (B) is also found in the spectrum obtained after digestion of the LTC_4-labeled protein (C) because of the relatively low cross-linking efficiency of MRP1 by LTC_4.

Mass spectrometric analysis of ligand binding sites of photolabeled proteins is often not possible because of low photolabeling efficiency by the ligand. However, current techniques can often overcome this limitation, and our study shows that this is the case, at least to a significant degree, for analysis of LTC_4-labeled MRP1. The six candidate LTC_4-modified MRP1 peptide fragments identified here are found in several different regions of the transporter with respect to its primary structure and include the COOH-proximal region of CL3 (peptide 260–274), TM6 (peptide 320–331), TM7 (peptide 372–385), TM10 and its cytosolic juxtamembrane region (peptide 546–553), and TM17 and its cytosolic juxtamembrane region (peptides 1233–1255 and 1248–1264) (Fig. 6). Thus, at least a portion of all candidate LTC_4-modified MRP1 peptides is predicted to be intracellular or in relatively proximity to the membrane-cytosol interface of the protein, in agreement with this region being an initial contact site of LTC_4.

To a significant extent, the sequence assignments of the LTC_4-modified peptides identified here are consistent with previous studies of wild-type and mutant MRP1 proteins. For example, more of the LTC_4-modified candidate peptides are found in the NH_2-proximal half of MRP1 than the COOH-proximal half, in agreement with our earlier finding that the two halves of MRP1 are differentially photolabeled by [^{3}H]LTC_4 (Qian et al., 2001). Furthermore, residues 1 to 204 were not found in any of the candidate peptides consistent with studies from several groups, demonstrating that the first MSD of MRP1 is not necessary for binding or transport of LTC_4 (Bakos et al., 1998; Lee and Altenberg, 2003a). On the other hand, although peptide 260 to 274 is located in the COOH-proximal half of CL3, a region previously suggested to be necessary for LTC_4 binding (and transport) and to contain a GSH binding site (Ren et al., 2001), we have found no evidence that residues NH_2 proximal to 281 could be directly photolabeled by this cysteinyl leukotriene (Westlake et al., 2003). Furthermore, deletion of residues 261 to 279 caused only a 30% decrease in LTC_4 transport activity, and mutation of Pro^{272} in this region had no effect at all (Ito et al., 2003). Further study is clearly needed to resolve this apparent discrepancy.

Identification of amino acids 320 to 331 as an LTC_4-modified peptide is consistent with earlier reports demonstrating the critical importance of TM6 for LTC_4 binding and transport. Thus, Bao et al. (2005) showed that replacement of TM6 (amino acids 320–337) with a poly-Ala chain abolishes LTC_4 transport by MRP1. Furthermore, we have shown that mutation of Lys^{332} immediately adjacent to the candidate TM6 peptide selectively eliminates LTC_4 binding and transport (Haimeur et al., 2002, 2004a). Together, the data support the idea that residues in TM6 can form direct contacts with

TABLE 2
Candidate LTC_4-modified peptide fragments of MRP1 identified by MALDI-TOF mass spectrometry

Protease	LTC_4-Modified Peptide	Corresponding Unmodified Peptide	Matched Theoretical Unmodified Peptide	Mass Accuracy (%)	Modified Peptide	Candidate Peptide Sequence	Predicted MRP1 Domain
	$[M + H^+]$ (m/z)	$[M + H^+]$ (m/z)	$[M + H^+]$ (m/z)				
V8 + tryp	2528.41	1902.01	1901.05	0.048		^{260}NWKKECAKTRKQPVK^{274}	CL3
Chymo + tryp	2129.02	1503.40	1503.70	−0.019		^{320}TFGPYFLMSFFF^{331}	TM6
Tryp + chymo	2316.73	1691.98	1692.80	−0.048		^{372}VTACLQTLVLHQYF^{385}	TM7
Chymo	1494.35	868.63	868.42	0.024		^{546}SAVGTFTW^{553}	CL5/TM10
V8 + chymo	3365.11	2739.74	2739.30	0.016	Met-Ox	^{1233}SVSYSLQVTTYLNWLVRMSSEME^{1255}	TM17
Chymo	2590.42	1964.07	1963.99	0.004		^{1248}VRMSSEMETNIVAVERL^{1264}	TM17 cytoplasmic interface

Chymo, chymotrypsin; tryp, trypsin; V8, protease V8; Met-ox, partial oxidation of methionine residues.

LTC_4. However, further studies using more sophisticated methods such as MALDI-tandem mass spectrometry technology for fragmentation studies of the LTC_4-labeled peptides are needed to determine definitively if this is the case.

The identification of peptide 372 to 385 as a candidate LTC_4-modified peptide represents the first time that TM7 has been implicated in LTC_4 binding by MRP1. However, our atomic homology models of MRP1 place TM7 in proximity to TM12, TM16, and TM17 (Campbell et al., 2004), and the latter two TMs are known to contain a significant number of mutation-sensitive residues with respect to LTC_4 binding and transport (see below). Thus, it is possible that TM7 may be photolabeled by LTC_4 by virtue of its proximity to the photoreactive region of the LTC_4 molecule rather than by any of its component amino acids directly contributing to the high-affinity binding of this substrate. On the other hand, candidate LTC_4-modified MRP1 peptide 546 to 553 is predicted to be proximal to the cytoplasmic interface of TM10, and this region has been identified in several studies as being important for binding and transport of LTC_4 as well as for binding of several photoaffinity analogs of a number of different compounds (Daoud et al., 2001; Koike et al., 2002).

The identification of LTC_4-modified peptides 1233 to 1255 and 1248 to 1264 that correspond to TM17 and its cytosolic juxtamembrane region was not surprising given that, like peptide 546 to 553, these overlapping peptides are part of a larger region that has been consistently reported by several groups to be critical for MRP1 transport activity as well as for the binding of several photoaffinity drug analogs (Daoud et al., 2001; Ito et al., 2001; Mao et al., 2002; Zhang et al., 2002; Ren et al., 2003). However, although we have shown that several polar residues within TM17 are important for MRP1 transport activity, mutations of these residues typically alter the substrate specificity of the transporter rather than abrogate its activity altogether. More notably, mutations of these residues do not affect LTC_4 binding or transport in any substantial way (Ito et al., 2001; Zhang et al., 2002). For example, mutations of Trp^{1246} eliminate transport of 17β-estradiol-D-17β-glucuronide and other glucuronide conjugates but leave LTC_4 transport essentially unchanged (Ito et al., 2001). Likewise, substitution of Tyr^{1243} with Phe causes a 70% reduction in 17β-estradiol-D-17β-glucuronide transport but has little effect on LTC_4 transport (Zhang et al., 2002). Supporting these findings are the observations of Bao et al. (2005), who recently reported that when amino acids 1228 to 1248 (TM17) are replaced with a poly-Ala chain, the mutant MRP1 retains the ability to transport LTC_4 as well as the wild-type protein. However, when residues in the COOH-proximal portion of the TM17 α-helix that extends beyond position 1248 into the cytoplasm are mutated, loss of transport activity becomes complete. Thus, in contrast to the minimal effect on LTC_4 transport caused by mutations of Trp^{1246} and Tyr^{1243}, even a conservative substitution of Arg^{1249} (Situ et al., 2004) (or Met^{1250}; C. Morean and S. P. C. Cole, unpublished observations) eliminates both binding and transport of LTC_4 as well as all other organic anions tested. Together, these observations suggest that the amino acid(s) in peptides 1248 to 1264 and 1233 to 1255 indicated in the present study to be cross-linked to LTC_4 are likely to reside in the cytoplasmic juxtamembrane position of TM17 between residues 1249 and 1264, rather than in the lipid bilayer itself. However, as mentioned above, further fragmentation analysis of the LTC_4-labeled peptides by MALDI-tandem mass spectrometry is needed to confirm this.

Karwatsky et al. (2005) recently photolabeled recombinant MRP1 containing multiple inserted epitope tags with [^{125}I]AALTC$_4$, an [^{125}I]iodoarylazido-derivatized analog of LTC_4, and after analysis of photolabeled tryptic fragments of the transporter, they concluded that the binding regions for LTC_4 included TM10 to 11 (amino acids 542–593) in the second MSD, and TM12 (amino acids 969-1013) and TM16 to 17 (amino acids 1203–1249) in the third MSD as well as the first MSD and NH_2-proximal portion of CL3 (amino acids 1–271). Our results obtained using the unmodified leukotriene C_4 seem to differ in several respects. For example, our study did not identify any candidate LTC_4-modified MRP1 peptides corresponding to residues in the first MSD (TM1–5) or in CL3 NH_2-proximal to position 260, or in TM12. On the other hand, Karwatsky et al. (2005) did not observe labeling of either the COOH-proximal portion of CL3 or TM6 or TM7 by [^{125}I]AALTC$_4$ as our present data suggest is the case with LTC_4.

There are a number of possible technical explanations for these differences that are related to the inherently different sensitivities and limitations of the different analytical methods used. However, the differences are also likely to be related to the fact that in the study of Karwatsky et al. (2005), as in many other photoaffinity labeling studies, an iodoarylazido derivative of LTC_4 was used (Sun et al., 1986). Thus, these investigators enhanced the photoreactivity of LTC_4 by introducing a bulky azido-benzoate group onto the γ-glutamyl residue of the GSH moiety of LTC_4. Because the γ-glutamyl residue is critical for the high affinity of LTC_4 for MRP1 (Leier et al., 1994), it is not surprising that this mod-

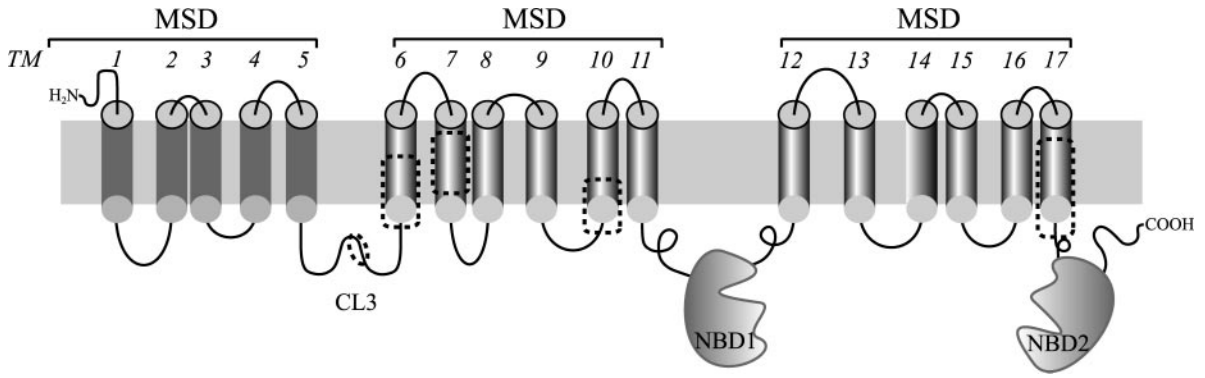

Fig. 6. Topological illustration showing location of candidate LTC_4-modified regions of MRP1 identified by MALDI-TOF mass spectrometry. The topological structure of MRP1 shown is based on a model derived by molecular dynamics simulations using the crystal structure of the bacterial lipid transporter MsbA as template (Campbell et al., 2004) as well as the HMMTOP 2.0 algorithm for predicting locations of TM helices of the first MSD (www.enzim.hu/hmmtop). The approximate locations of the candidate LTC_4-modified peptide sequences of MRP1 suggested by MALDI-TOF mass spectrometry of photolabeled protein are indicated by broken lines.

ification lowered the apparent affinity (K_m) of the organic anion substantially (Karwatsky et al., 2005), indicating that the chemical modification altered the binding characteristics of LTC_4. This difference in binding properties may also explain why LTC_4 preferentially photolabels the NH_2-terminal half of MRP1 (Qian et al., 2001), whereas [^{125}I]AALTC_4 preferentially photolabels the COOH-terminal half (Karwatsky et al., 2005). Thus, it is likely that the amino acid contacts for LTC_4 and [^{125}I]AALTC_4 in MRP1 are not precisely the same.

The mechanism of substrate transport by MRP1 is complex and not yet fully understood. However, it is generally accepted that the transport cycle is initiated by substrate binding that gives rise to a conformational change in MRP1 followed by sequential ATP binding to the NBDs and conformational change of the binding pocket, so that the substrate shifts from a high-affinity binding site to a low-affinity binding site facilitating its release on the other side of the membrane. The transport cycle is completed by hydrolysis of ATP (primarily at NBD2) and subsequent energy transfer from the NBDs to the TMs, and by release of ADP and restoration of the "resting" high-affinity state of the transporter (Higgins and Linton, 2004). Therefore, studies such as those described here provide only a static snapshot of LTC_4 binding by the transporter in its basal conformation. Ecker et al. (2004) recently showed by MALDI-TOF mass spectrometry that ATP binding increased the accessibility of the fifth TM helix of the bacterial ABC transporter LmrA to labeling by a photoactive ligand, whereas ATP hydrolysis had the opposite effect. Therefore, our future studies are directed toward determining whether the LTC_4-modified MRP1 peptide fragments (and individual amino acids) that can be identified by mass spectrometry differ at the different stages of the transport cycle of this ABC protein.

Acknowledgments

We thank Drs. Cai and Gros (McGill University) and Drs. Anass Haimeur and Alice Rothnie (Queen's University) for helpful advice and discussion. The technical assistance from Kathy Sparks is appreciated.

References

Bakos E, Evers R, Szakacs G, Tusnady GE, Welker E, Szabo K, de Haas M, van Deemter L, Borst P, Varadi A, et al. (1998) Functional multidrug resistance protein (MRP1) lacking the N-terminal transmembrane domain. *J Biol Chem* **273:**32167–32175.

Bao X, Chen Y, Lee SH, Lee SC, Reuss L, and Altenberg GA (2005) Membrane transport proteins with complete replacement of transmembrane helices with polyalanine sequences remain functional. *J Biol Chem* **280:**8647–8650.

Cai J and Gros P (2003) Overexpression, purification and functional characterization of ATP-binding cassette transporters in the yeast, *Pichia pastoris*. *Biochim Biophys Acta* **1610:**63–76.

Cai J, Daoud R, Georges E, and Gros P (2001) Functional expression of multidrug resistance protein 1 in *Pichia pastoris*. *Biochemistry* **40:**8307–8316.

Campbell JD, Koike K, Moreau C, Sansom MSP, Deeley RG, and Cole SPC (2004) Molecular modeling correctly predicts the functional importance of Phe^{594} in transmembrane helix 11 of the multidrug resistance protein, MRP1 (ABCC1). *J Biol Chem* **279:**463–468.

Chang XB, Hou YX, and Riordan JR (1997) ATPase activity of purified multidrug resistance-associated protein. *J Biol Chem* **272:**30962–30968.

Cole SPC, Bhardwaj G, Gerlach JH, Mackie JE, Grant CE, Almquist KC, Stewart AJ, Kurz EU, Duncan AMV, and Deeley RG (1992) Overexpression of a transporter gene in a multidrug resistant human lung cancer cell line. *Science (Wash DC)* **258:**1650–1654.

Dai YQ, Whittal RM, and Li L (1999) Two-layer sample preparation: a method for MALDI-MS analysis of complex peptide and protein mixtures. *Anal Chem* **71:** 1087–1091.

Daoud R, Julien M, Gros P, and Georges E (2001) Major photoaffinity drug binding sites in multidrug resistance protein 1 (MRP1) are within transmembrane domains 10–11 and 16–17. *J Biol Chem* **276:**12324–12330.

Ding Q, Xiao L, Xiong S, Jia Y, Que H, Guo Y, and Liu S (2003) Unmatched masses in peptide mass fingerprints caused by cross-contamination: an updated statistical result. *Proteomics* **3:**1313–1317.

Ecker G, Csaszar E, Kopp S, Plagens B, Holzer W, Ernst W, and Chiba P (2002) Identification of ligand-binding regions of P-glycoprotein by activated-pharmacophore photoaffinity labeling and matrix-assisted laser desorption/ionization-time-of-flight mass spectrometry. *Mol Pharmacol* **61:**637–648.

Ecker GF, Pleban K, Kopp S, Csaszar E, Poelarends GJ, Putman M, Kaiser D, Konings WN, and Chiba P (2004) A three-dimensional model for the substrate binding domain of the multidrug ATP binding cassette transporter LmrA. *Mol Pharmacol* **66:**1169–1179.

Eichacker LA, Granvogl B, Mirus O, Muller BC, Miess C, and Schleiff E (2004) Hiding behind hydrophobicity. Transmembrane segments in mass spectrometry. *J Biol Chem* **29:**50915–50922.

Falk E, Muller M, Huber M, Keppler D, and Kurz G (1989) Direct photoaffinity labeling of leukotriene binding sites. *Eur J Biochem* **186:**741–747.

Gao M, Yamazaki M, Loe DW, Westlake CJ, Grant CE, Cole SPC, and Deeley RG (1998) Multidrug resistance protein: identification of regions required for active transport of leukotriene C_4. *J Biol Chem* **273:**10733–10740.

Glish GL and Vachet RW (2003) The basics of mass spectrometry in the twenty-first century. *Nat Rev Drug Discov* **2:**140–150.

Haimeur A, Conseil G, Deeley RG, and Cole SPC (2004a) Mutations of charged amino acids in or proximal to the transmembrane helices of the second membrane spanning domain differentially affect the substrate specificity and transport activity of the multidrug resistance protein, MRP1 (ABCC1). *Mol Pharmacol* **65:** 1375–1385.

Haimeur A, Conseil G, Deeley RG, and Cole SPC (2004b) The MRP-related and BCRP/ABCG2 multidrug resistance proteins: biology, substrate specificity and regulation. *Curr Drug Metab* **5:**21–53.

Haimeur A, Deeley RG, and Cole SPC (2002) Charged amino acids in the sixth transmembrane helix of multidrug resistance protein 1 (MRP1/ABCC1) are critical determinants of transport activity. *J Biol Chem* **277:**41326–41333.

Higgins CF and Linton KJ (2004) The ATP switch model for ABC transporters. *Nat Struct Mol Biol* **11:**918–926.

Hipfner DR, Almquist KC, Leslie EM, Gerlach JH, Grant CE, Deeley RG, and Cole SPC (1997) Membrane topology of the multidrug resistance protein, MRP: a study of glycosylation site mutants reveals an extracytosolic NH_2-terminus. *J Biol Chem* **272:**23623–23630.

Hipfner DR, Almquist KC, Stride BD, Deeley RG, and Cole SPC (1996) Location of a protease-hypersensitive region in the multidrug resistance protein (MRP) by

mapping of the epitope of MRP-specific monoclonal antibody QCRL-1. *Cancer Res* **56:**3307–3314.
Ito K, Olsen SL, Qiu W, Deeley RG, and Cole SPC (2001) Mutation of a single conserved tryptophan in multidrug resistance protein 1 (MRP1/ABCC1) results in loss of drug resistance and selective loss of organic anion transport. *J Biol Chem* **276:**15616–15624.
Ito K-I, Weigl KE, Deeley RG, and Cole SPC (2003) Mutation of proline residues in the NH_2-terminal region of the multidrug resistance protein, MRP1 (ABCC1): effects on protein expression, membrane localization and transport function. *Biochim Biophys Acta* **1615:**103–114.
Karwatsky JM, Leimanis M, Cai J, Gros P, and Georges E (2005) The leucotriene C_4 binding sites in multidrug resistance protein 1 (ABCC1) include the first membrane multiple spanning domain. *Biochemistry* **44:**340–351.
Koike K, Conseil G, Leslie EM, Deeley RG, and Cole SPC (2004) Identification of proline residues in the core cytoplasmic and transmembrane regions of multidrug resistance protein 1 (MRP1/ABCC1) important for transport function, substrate specificity and nucleotide interactions. *J Biol Chem* **279:**12325–12336.
Koike K, Oleschuk CJ, Haimeur A, Olsen SL, Deeley RG, and Cole SPC (2002) Multiple membrane associated tryptophan residues contribute to the transport activity and substrate specificity of the human multidrug resistance protein, MRP1. *J Biol Chem* **277:**49495–49503.
Lee SH and Altenberg GA (2003a) Expression of functional multidrug-resistance protein 1 in *Saccharomyces cerevisiae*: effects of N- and C-terminal affinity tags. *Biochem Biophys Res Commun* **306:**644–649.
Lee SH and Altenberg GA (2003b) Transport of leukotriene C_4 by a cysteine-less multidrug resistance protein 1 (MRP1). *Biochem J* **370:**357–360.
Leier I, Jedlitschky G, Buchholz U, Cole SPC, Deeley RG, and Keppler D (1994) The MRP gene encodes an ATP-dependent export pump for leukotriene C_4 and structurally related conjugates. *J Biol Chem* **269:**27807–27810.
Leslie EM, Deeley RG, and Cole SPC (2005) Multidrug resistance proteins in toxicology: role of P-glycoprotein, MRP1, MRP2 and BCRP (ABCG2) in tissue defense. *Toxicol Appl Pharmacol* **204:**216–237.
Loe DW, Almquist KC, Deeley RG, and Cole SPC (1996) Multidrug resistance protein (MRP)-mediated transport of leukotriene C_4 and chemotherapeutic agents in membrane vesicles: demonstration of glutathione-dependent vincristine transport. *J Biol Chem* **271:**9675–9682.
Mao Q, Conseil G, Gupta A, Cole SPC, and Unadkat JD (2004) Functional expression of the human breast cancer resistance protein in *Pichia pastoris*. *Biochem Biophys Res Commun* **320:**730–737.
Mao Q, Deeley RG, and Cole SPC (2000) Functional reconstitution of substrate transport by purified multidrug resistance protein MRP1 (ABCC1) in phospholipid vesicles. *J Biol Chem* **275:**34166–34172.
Mao Q, Qiu W, Weigl KE, Lander PA, Tabas LB, Shepard RL, Dantzig AH, Deeley RG, and Cole SPC (2002) GSH-dependent photolabeling of multidrug resistance protein MRP1 (ABCC1) by [^{125}I]-LY475776: evidence of a major binding site in the COOH-proximal membrane spanning domain. *J Biol Chem* **277:**28690–28699.
Mao Q, Leslie EM, Deeley RG, and Cole SPC (1999) ATPase activity of purified and reconstituted multidrug resistance protein (MRP1) from drug-selected H69AR cells. *Biochim Biophys Acta* **1461:**69–82.
Muller M, Meijer C, Zaman GJ, Borst P, Scheper RJ, Mulder NH, de Vries EG, and Jansen PL (1994) Overexpression of the gene encoding the multidrug resistance-associated protein results in increased ATP-dependent glutathione S-conjugate transport. *Proc Natl Acad Sci USA* **91:**13033–13037.
Muller M, Yong M, Peng XH, Petre B, Arora S, and Ambudkar SV (2002) Evidence for the role of glycosylation in accessibility of the extracellular domains of human MRP1 (ABCC1). *Biochemistry* **41:**10123–10132.
Pleban K, Kopp S, Csaszar E, Peer M, Hrebicek T, Rizzi A, Ecker GF, and Chiba P (2005) P-glycoprotein substrate binding domains are located at the transmembrane domain/transmembrane domain interfaces: a combined photoaffinity labeling-protein homology modeling approach. *Mol Pharmacol* **67:**365–374.
Qian YM, Qiu W, Gao M, Westlake CJ, Cole SPC, and Deeley RG (2001) Characterization of binding of leukotriene C_4 by human multidrug resistance protein 1: evidence of differential interactions with NH_2- and COOH-proximal halves of the protein. *J Biol Chem* **276:**38636–38644.
Quach TT, Li N, Richards DP, Zheng J, Keller BO, and Li L (2003) Development and applications of in-gel CNBr/tryptic digestion combined with mass spectrometry for the analysis of membrane proteins. *J Proteome Res* **2:**543–552.
Reid GE (2004) Characterization of proteins by mass spectrometry, in *Purifying Proteins for Proteomics* (Simpson RJ ed) pp 489–516, Cold Spring Harbor Laboratory Press, Cold Spring Harbor, NY.
Ren XQ, Furukawa T, Aoki S, Nakajima T, Sumizawa T, Haraguchi M, Chen ZS, Kobayashi M, and Akiyama S (2001) Glutathione-dependent binding of a photoaffinity analog of agosterol A to the C-terminal half of human multidrug resistance protein. *J Biol Chem* **276:**23197–23206.
Ren XQ, Furukawa T, Aoki S, Sumizawa T, Haraguchi M, Che XF, Kobayashi M, and Akiyama S (2003) Localization of the GSH-dependent photolabelling site of an agosterol A analog on human MRP1. *Br J Pharmacol* **138:**1553–1561.
Situ D, Haimeur A, Conseil G, Sparks KE, Zhang D, Deeley RG, and Cole SPC (2004) Mutational analysis of ionizable residues proximal to the cytoplasmic interface of membrane spanning domain 3 of the multidrug resistance protein, MRP1 (ABCC1): glutamate 1204 is important for both the expression and catalytic activity of the transporter. *J Biol Chem* **279:**38871–38880.
Sun FF, Chau L-Y, Spur B, Corey EJ, Lewis RA, and Austen KF (1986) Identification of a high affinity leukotriene C_4-binding protein in rat liver cytosol as glutathione S-transferase. *J Biol Chem* **261:**8540–8546.
Van Montfort BA, Doeven MK, Canas B, Veenhoff LM, Poolman B, and Robillard GT (2002) Combined in-gel tryptic digestion and CNBr cleavage for the generation of peptide maps of an integral membrane protein with MALDI-TOF mass spectrometry. *Biochim Biophys Acta* **1555:**111–115.
Washburn MP, Wolters D, and Yates JR (2001) Large-scale analysis of the yeast proteome by multidimensional protein identification technology. *Nat Biotechnol* **19:**242–247.
Westlake CJ, Qian YM, Gao M, Vasa M, Cole SPC, and Deeley RG (2003) Identification of the structural and functional boundaries of the multidrug resistance protein 1 cytoplasmic loop 3. *Biochemistry* **42:**14099–14113.
Wijnholds J, Evers R, van Leusden MR, Mol CA, Zaman GJ, Mayer U, Beijnen JH, van der Valk M, Krimpenfort P, and Borst P (1997) Increased sensitivity to anticancer drugs and decreased inflammatory response in mice lacking the multidrug resistance-associated protein. *Nat Med* **3:**1275–1279.
Yang R, Cui L, Hou YX, Riordan JR, and Chang XB (2003) ATP binding to the first nucleotide binding domain of multidrug resistance-associated protein plays a regulatory role at low nucleotide concentration, whereas ATP hydrolysis at the second plays a dominant role in ATP-dependent leukotriene C_4 transport. *J Biol Chem* **278:**30764–30771.
Zhang D, Cole SPC, and Deeley RG (2002) Determinants of the substrate specificity of multidrug resistance protein 1 (MRP1): role of amino acid residues with hydrogen bonding potential in predicted transmembrane helix 17. *J Biol Chem* **277:**20934–20941.
Zhang D-W, Nunoya K, Vasa M, Gu HM, Theis A, Cole SPC, and Deeley RG (2004) Transmembrane helix 11 of multidrug resistance protein 1 (MRP1/ABCC1): identification of polar amino acids important for substrate specificity and binding of ATP at nucleotide binding domain 1. *Biochemistry* **43:**9413–9425.

Address correspondence to: Dr. Susan P. C. Cole, Cancer Research Laboratories, 3rd Floor Botterell Hall, Queen's University, Kingston, ON, Canada K7L 3N6. E-mail: coles@post.queensu.ca